Article ID: 1006-8775(2009) 01-0204-06

THE THEORY OF MOIST POTENTIAL VORTICITY AND ITS APPLICATION IN THE DIAGNOSIS OF TYPHOON RAINFALL AND INTENSITY

DENG Guo (邓 国)[1], GAO Shou-ting (高守亭)[2]

(1. National Meteorological Center, Beijing 100081 China; 2. Institute of Atmospheric Physics, Chinese Academy of Sciences, Beijing 100029 China)

Abstract: This paper tests the impacts of cloud-induced mass forcing on the moist potential vorticity (MPV) anomaly associated with torrential rains caused by Typhoon No.9914 (Dan) by using fine model simulation data outputted by the Fifth-Generation NCAR / Penn State Mesoscale Model (MM5). The diagnostic results show that the positive MPV anomaly region, which is obtained by integrating the MPV from 600 hPa to 300 hPa in the vertical, roughly coincides with the precipitation at their synchronous stages either in position or in the distribution pattern, and the maximum positive MPV area of Dan is located mainly between 600 hPa and 300 hPa, which is much higher than torrential rain cases. Further analyses also showed that the value of positive MPV anomaly increased or decreased with the development of Dan, and the positive MPV anomaly may also be served as a tracer to indicate the evolution of tropical cyclone intensity.

Key words: moist potential vorticity; typhoon; mass forcing

CLC number: P457.6 **Document code:** A **doi:** 10.3969/j.issn.1006-8775.2009.02.009

1 INTRODUCTION

The general potential vorticity (PV) concept is given by Ertel[1]. Some historical notes and reviews are given in Haynes and Mcintyre[2]. Indeed, PV analysis, which has become well established since the major work of Hoskins et al. [3], provided a powerful tool for investigation of such a process. PV concepts have been used to describe various processes in idealized tropical cyclones with considerable success[4,5]. Shapiro and Franklin[6] have studied the three-dimensional structure of PV in Hurricane Gloria of 1985, including the storm-core region. Molinari et al. [7] studied the interaction of Hurricane Elena with the upper-tropospheric trough by using the PV framework. Although there have been so many studies on tropical cyclones (hurricanes and typhoons), by introducing the potential vorticity concept, the formula of dry potential vorticity in most of the work was inadquately used to study the tropical cyclones with the evident moist saturated air. Even if the moist potential vorticity (MPV) was used [8], they ignored the effect of heat and mass forcings. Deng et al. [9] study the impact of boundary action on typhoon structure. Gao et al. [10-13] derived a MPV tendency equation with the cloud-induced mass forcing and applied to a torrential rain event over the Changjiang River-Huaihe River Valleys during 26–30 June 1999. Their results show that positive anomalies are located mainly between 850 hPa and 500 hPa, while the maximum MPV, maximum positive tendency of the MPV, and maximum surface rainfall are nearly collocated. In their further researches, Gao et. al [14-16] put forward the concept of generalized MPV which considers the fact that condensation always takes place even if the relative humidity is under 100%. Although both the torrential rainfall and typhoon share the same character of near saturation, there are many differences in other aspects: dynamics, thermodynamics, structure (especially the structure of moisture and rainband), evolution, etc. Therefore, the question is that in addition to the relation of MPV generation to the solenoid term in the potential

Received date: 2009-03-28; **revised date:** 2009-09-10

Foundation item: State Key Development Program for Basic Research of China (2009CB421505); National Natural Science Foundation of China (40505009); NMC-TIGGE Program (GYHY200706001); Project of State Key Laboratory of Severe Weather (2008LASW-A01)

Biography: DENG Guo, PhD, mainly undertaking the research on ensemble forecasts, tropical cyclones and mesoscale dynamics.

E-mail for correspondence author: deng719@cma.gov.cn

vorticity equation, are there any MPV anomalies in the typhoon system which are induced by mass forcings? It needs further research on the character of MPV in tropical cyclones through the theoretical, diagnostic analysis and the simulation of MPV. For this purpose, we are motivated to probe into the questions by analyzing the case of Dan that occurred in the West Pacific in 1999. The MPV anomalies induced by the mass forcing are diagnosed from the numerical simulation data provided by MM5.

This article is organized as follows: The potential vorticity anomaly with heat and mass forcings is further reviewed briefly in section 2 according to the character of typhoons. Section 3 gives a brief description of simulation results of the research done on Dan. The potential vorticity anomalies of Dan are given in section 4, and a summary is presented in section 5.

2 MOIST POTENTIAL VORTICITY EQUATION WITH MASS FORCINGS IN TYPHOON

2.1 *Brief review of MPV equation with mass forcing*

In the study of typhoon systems, the change of the mass field is not only caused by divergence and convergence of the environmental field, but also affected by significant mass reduction induced by intensive precipitation. Therefore, when the MPV notion is used to study the typhoon system, mass forcing must be considered. In order to study the MPV anomalies caused by mass forcing in the typhoon system, it is described briefly in this section.

The vorticity equation, continuity equation and thermodynamic equation in Cartesian coordinates are as follows:

$$\frac{d\boldsymbol{\omega}_a}{dt} = (\boldsymbol{\omega}_a \cdot \nabla)\mathbf{V} - \boldsymbol{\omega}_a \nabla \cdot \mathbf{V} - \nabla \wedge \mathbf{F}, \quad (1)$$

$$\frac{d\rho}{dt} + \rho\nabla \cdot \mathbf{V} = Q_m, \quad (2)$$

$$\frac{d\theta_e}{dt} = \dot{\psi}, \quad (3)$$

where ω_a represents the absolute vorticity and $\mathbf{F}$ is the term associated with friction. The mass forcing Q_m, caused by the intensive precipitation, and heat forcing $\dot{\psi}$, induced by latent heat release of ice-water phase transformation, are added to the right hand side of Eqs. (2) and (3) respectively. Then, the potential vorticity equation with mass forcing is given as

$$\frac{d}{dt}\left(\frac{\omega_a \cdot \nabla\theta_e}{\rho}\right) = \frac{1}{\rho}\omega_a \cdot \nabla\frac{d\theta_e}{dt} - \frac{Q_m}{\rho}\left(\frac{\omega_a \cdot \nabla\theta_e}{\rho}\right) - \frac{1}{\rho}\nabla\theta_e \cdot \nabla \wedge \mathrm{F}, \quad (4)$$

where $\frac{\omega_a \cdot \nabla\theta_e}{\rho}$ is the moist Ertel potential vorticity and the deduction process can be found in Gao et al. [11, 12]. By utilizing Eq. (3), Eq. (4) can be further written as

$$\frac{d}{dt}\left(\frac{\omega_a \cdot \nabla\theta_e}{\rho}\right) = \frac{1}{\rho}\omega_a \cdot \nabla\dot{\psi} - \frac{Q_m}{\rho}\left(\frac{\omega_a \cdot \nabla\theta_e}{\rho}\right) - \frac{1}{\rho}\nabla\theta_e \cdot \nabla \wedge \mathrm{F}. \quad (5)$$

On the right hand side of Eq. (5), the first term reflects the effect of heat forcing, the second term the effect of mass forcing and the third term the effects of solenoid and friction.

2.2 *MPV anomalies in typhoon*

By dividing the last term in Eq. (5) into two terms, one being the pressure gradient forcing and the other being the frictional forces, Eq. (5) can then be further written as

$$\frac{d}{dt}\left(\frac{\omega_a \cdot \nabla\theta_e}{\rho}\right) = \frac{1}{\rho}\omega_a \cdot \nabla\dot{\psi} - \frac{Q_m}{\rho}\left(\frac{\omega_a \cdot \nabla\theta_e}{\rho}\right) + \nabla\theta_e \cdot \left(\frac{\nabla\rho \times \nabla p}{\rho^3}\right) + \frac{1}{\rho}\nabla\theta_e \cdot \nabla \wedge \tau, \quad (6)$$

where τ represents any frictional forces and other variables have their usual meaning. In the free atmosphere, the flow may be assumed frictionless, with $\tau = 0$; the third term in Eq. (6), $\nabla\theta_e \cdot \left(\frac{\nabla\rho \times \nabla p}{\rho^3}\right)$, is zero, if the flow is either two-dimensional or saturated (e.g., Bennetts and Hoskins[17]; Cao and Cho, 1995[18]), because in the latter case, θ_e is a function of density ρ and pressure p only. For the case of Dan, above the level of lifted condensation, the flow is saturated and so the term associated with solenoid in Eq. (6) becomes namely zero. Therefore, in the saturated region of Dan, Eq. (6) may be rewritten as

$$\frac{d}{dt}\left(\frac{\omega_a \cdot \nabla\theta_e}{\rho}\right) = \frac{1}{\rho}\omega_a \cdot \nabla\dot{\psi} - \frac{Q_m}{\rho}\left(\frac{\omega_a \cdot \nabla\theta_e}{\rho}\right). \quad (7)$$

In this paper, as the impact of mass forcing to MPV was the key factor, the heat forcing was neglected. So Eq. (7) may be further written as:

$$\frac{d}{dt}\left(\frac{\omega_a \cdot \nabla\theta_e}{\rho}\right) \approx -\frac{Q_m}{\rho}\left(\frac{\omega_a \cdot \nabla\theta_e}{\rho}\right). \quad (8)$$

Therefore, Eq. (8) indicates that the MPV anomaly is mainly caused by mass forcing from precipitation.

To test the efficiency of the mass forcing theory in typhoon systems, a typical typhoon precipitation case (Dan) is selected and its numerical simulation with the mesoscale model PSU/NCAR MM5 is diagnosed in the next section.

3 NUMERICAL SIMULATIONS

Dan is one of the most severe tropical cyclones during the past 40 years that ever hit Fujian province and caused great causalities. To simulate its development and landfall process, a double nested, two-way interactive version of the PSU/NCAR MM5 (v3.5) is utilized. The two domains have the (x, y) dimensions of 130 ×156 and 184 × 214 grid points, with the grid sizes of 36 and 12 km, respectively. There are 26 σ-levels in the vertical. The two domains use the same schemes for physical processes: The Bett-Meller scheme is used for cumulus parameterization and the Graupel scheme is selected in cloud microphysics, together with the Blackadar planetary boundary layer scheme, a cloud-radiation interaction scheme and a shallow convective scheme [14]. The initial conditions at 0000 UTC 7 October 1999 are obtained from the ECMWF's 2.5°× 2.5° global analysis data, and then integrated for 72 h, valid at 0000 UTC 10 October 1999.

Fig. 1 compares the tracks of Dan during the 72-h simulations (dashed line in Fig.1) to the best track (the observations, solid line in Fig. 1). It is obvious that the simulation describes the development and landfall processes of the typhoon quite well during the 72-h simulation and test. The simulated accumulated precipitation (Fig. 2b) is comparable to the observation (Fig. 2a) in both the amount and center, and Fig. 2 indicates that the simulated rainfall region and rainfall amount are similar to those of observation. For some other important indexes to evaluate the effect of simulation/forecast of typhoons against the observation, such as the simulated track, the simulated minimum central pressures (Fig. 3) and the maximum surface wind (omitted) are all closer to the observed value. The differences between the simulated minimum centre pressure and the observed values in Fig. 3 are not more than 5 hPa from 0800 UTC 7 October, which shows that the simulated intensity is close to the observation. In summary, the simulation with the typhoon vortex exhibits considerable skill in reproducing the observed track, intensity and inner-core structures of the storm. In particular, the simulated asymmetry in the precipitation structure has important applications with respect to the improvement of quantitative precipitation forecasts and severe wind warnings for landfall typhoons. For further details on the case study of Dan, the reader is referred to the work of Deng et al.[9]. The successful simulation of this typhoon case lays the foundation for testing the relationship of MPV anomaly to its precipitation.

From the formula in section 2, it could be concluded that if there are local anomalies of the potential vorticity in the saturated region of typhoon system, the anomalies must be mainly caused by the mass forcing related to precipitation. Cross sections of the MPV (Fig. 4) show that the positive MPV anomaly by cloud-induced mass forcing during heavy rains mainly exists between 600 hPa and 300 hPa and the maximum value area is located between 500 hPa and 400 hPa. This result basically conforms to Gao's analysis[10]. However, there is some difference between the two results: Gao's aim is on Meiyu precipitation while this case is for typhoon precipitation; therefore, the positive MPV anomaly area is somewhat higher in Dan than that in Meiyu torrential rain. The reason may be that the convection developing in a typhoon system is much stronger than any other precipitation systems, and in turn corresponds to a higher positive MPV anomaly area.

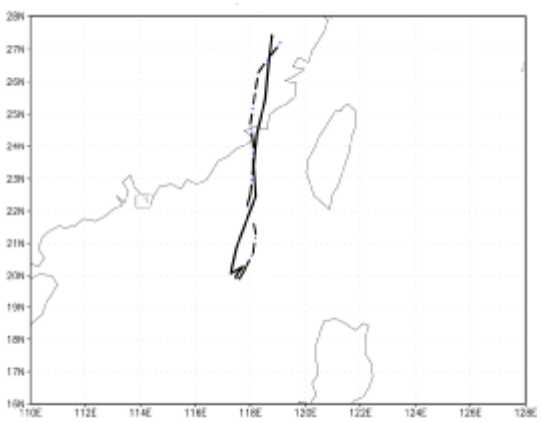

Fig.1 Comparison of simulated typhoon track and observation (observation: solid line; simulation: dashed line).

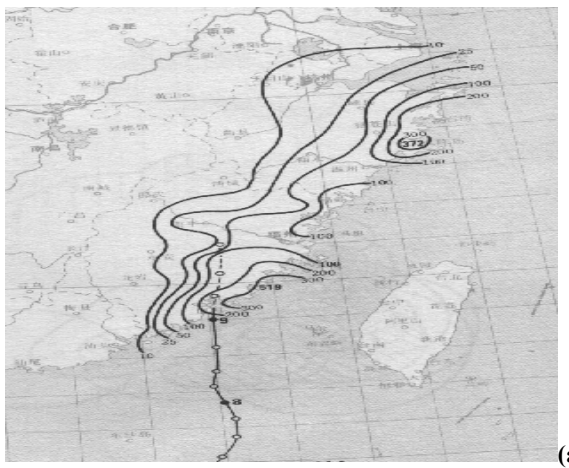

(a)

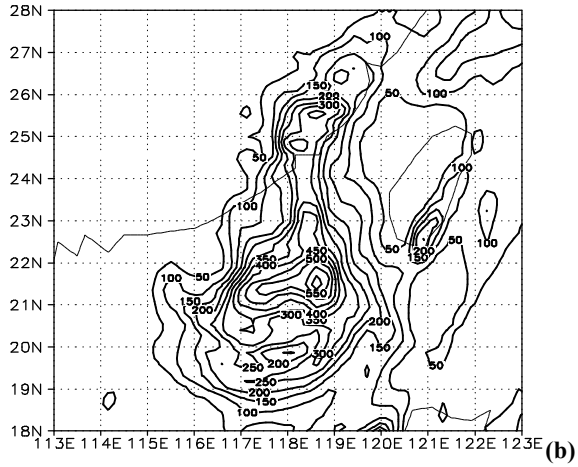

Fig.2 Comparison of observed precipitation (a) and simulated precipitation (b). (unit in mm)

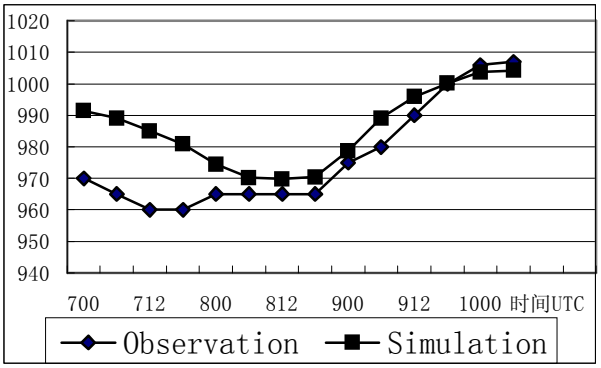

Fig.3 Comparison of simulated typhoon's minimum sea level pressure and observation. (unit in hPa)

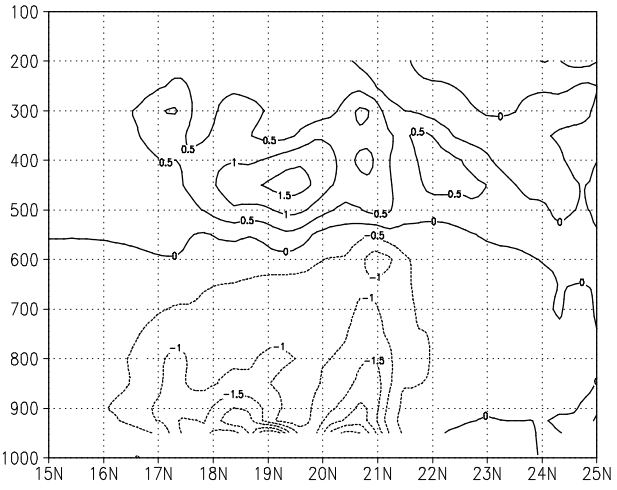

Fig.4 Cross section of MPV along 118ºE (0600 UTC 7 October 1999), solid lines: area where MPV>0, dashed lines: area where MPV<0.

To test the relationship between MPV precipitation, we pick up three different simulation periods to indicate different development stages of the typhoon: the premature developed stage, the full development stage and the landfall stage. At each stage, the MPV anomaly is compared to corresponding precipitation to show their correlation. Figs. 5, 6 and 7 are comparisons between 3-hr accumulated precipitation and the corresponding integrated MPV between 600 hPa and 300 hPa. The reason why we calculate the integrated MPV between 600 hPa and 300 hPa lies in that at which levels the positive MPV value area is located (see the distribution of positive MPV in Fig. 4.

At the prematurely developed stage, it is seen that the distribution of both the integrated MPV anomaly (contours in Fig. 5a, b) and 3-hr accumulated precipitation (shaded in Fig. 5a, b) shows the character of an asymmetric structure: the maximum precipitation is located in the north of Dan and the maximum value could reach 100 mm; correspondingly, the distribution of the integrated MPV shares a similar form to that of rainband: a large value area of integrated MPV almost overlaps with a large precipitation area in general, although the two maximum centers are not collocated point to point.

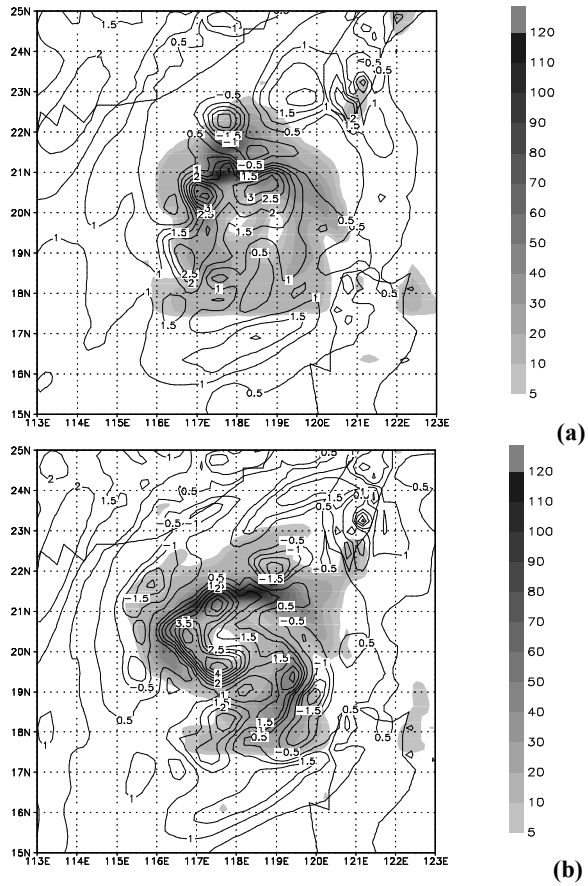

Fig.5 Integrated MPV corresponding to 3-hour accumulated precipitation (unit in PVU, 1 PVU=1.0×10^{-6} $m^2 \cdot s^{-1} \cdot K \cdot kg^{-1}$): from 0300 UTC to 0600 UTC (a) and from 0600 UTC to 0900 UTC (b) on 7 October.

At the fully developed stage of Dan (Fig. 6), the values of integrated MPV increase with typhoon

intensity and the maximum integrated MPV(contour in Fig. 6a, b) could reach 5.5 PVU, a little larger than in Dan's premature stage, when the maximum integrated MPV is about 3.5 PVU. However, the corresponding precipitation does not increase accordingly. Fortunately, it shows that the distribution of the integrated MPV and 3-hr accumulated precipitation (shaded in Fig. 6a, b) collated well generally. In detail, at 1800 UTC 7 October, the maximum precipitation is located on the right side of Dan, and so is the distribution of integrated MPV (Fig. 6a). At 2100 UTC 7 October, a large typhoon precipitation area is dot-shaped, with a low value area in the southwest; correspondingly, a large integrated positive MPV area covers the similar area (Fig. 6b). It is notable that in the eyewall area of Dan, the precipitation is very small due to dry, ascending air, and the corresponding relationship between MPV and precipitation is not strong in this area. Another notable area is that besides the good correlation of value and distribution between the two factors, a better distribution is indicated in the high gradient area of the integrated MPV and precipitation (see Figs. 5, 6).

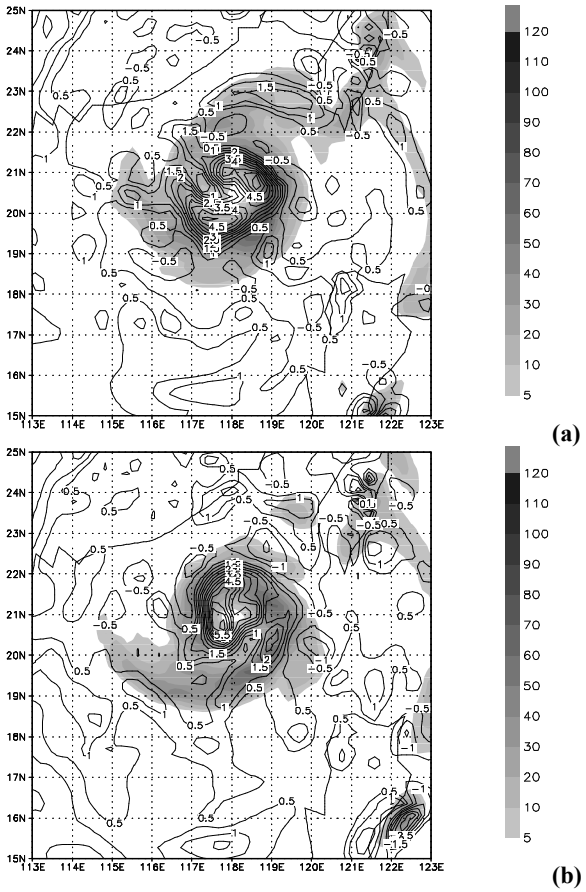

Fig.6 3-hour accumulated precipitation and corresponding integrated MPV: from 1500 UTC to 1800 UTC (a) and from 1800 UTC to 2100 UTC(b), 7 October.

At the landfall stage of Dan, the value of integrated MPV decreases with typhoon intensity due to terrain friction and lose of water vapor (see Fig. 7) and the maximum integrated MPV (contours in Fig. 7a, b) decreases to around 4 PVU, somewhat lower than in Dan's mature stage. However, the corresponding precipitation (shaded in Fig. 7a, b) increases due to terrain effect. Similar to previous stages, the distribution of the integrated MPV and 3-hr accumulated precipitation still collates well generally, especially the association of high gradient areas of integrated MPV with large precipitation areas.

4 SUMMARY AND DISCUSSION

This paper tests the impacts of cloud-induced mass forcing on the development of the moist potential vorticity (MPV) anomaly associated with typhoon torrential rains by using MM5-output data. Unlike previous studies of mass forcing—which make use of coarse analysis data—this research diagnoses the MPV results based on high resolution model simulations. Likewise, these results indicate that the mass forcing, generated by the intensive precipitation of Dan, indeed generates the anomalies of MPV, with the positive MPV anomaly located between 600 hPa and 300 hPa. From the diagnostic studies of this case, we can find that the distribution of vertical integrated positive MPV roughly coincides with the precipitation at their synchronous stages either in position or in the distribution pattern.

The maximum positive MPV area of Dan is located mainly between 600 hPa and 300 hPa, which is much higher than that for the Meiyu front torrential rain cases. This may be attributed to the fact that the convection of Dan was much more severe than in normal precipitation systems. The maximum MPV anomaly and corresponding precipitation area of Dan does not match point to point (especially in the eyewall area), which may be caused by the strong wind movement in tropical cyclones.

It is also found that the value of positive MPV anomaly increased or decreased with the development of Typhoon Dan. At the prematurely developed stage, the value of positive MPV is relatively small. Then at the fully developed stage, it reaches its maximum. At the landfall stage, the intensity of typhoon decreases, and the MPV decreases correspondingly. Therefore, the positive MPV may serve as a passive tracer to indicate the evolution of Dan's intensity.

Although we get roughly corresponding relationships between the MPV anomaly and precipitation, only the factor of mass forcing is considered while some other factors, such as forcings induced by heat, horizontal wind shear, and vertical

motion, etc, are not derived here. Hence it is impossible to match with each other very well, which deserves further exploration.

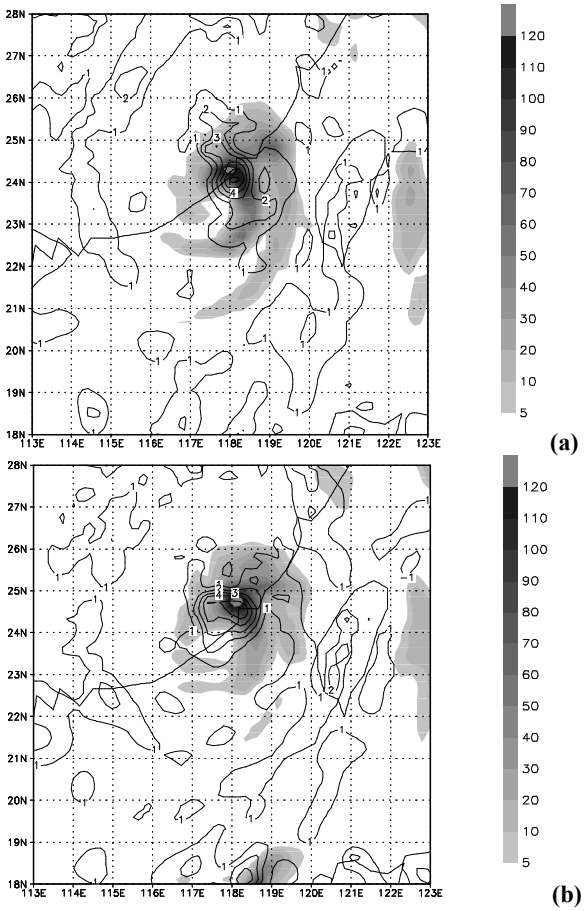

Fig.7 3-hour accumulated precipitation and corresponding integrated MPV: from 2100 UTC to 2400 UTC 8 October (a) and from 0000 UTC to 0300 UTC 9 October (b).

REFERENCES:

[1] ERTEL H. Ein Neuer gydrodynamischer Wirbelsatz [J]. Me. Z., 1942, 59: 277-281.
[2] HAYNES P H, MCINTYRE M E. On the Conservation and Impermeability Theorems for Potential Vorticity [J]. J. Atmos. Sci., 1990, 47: 2021-2031.
[3] HOSKINS B J, MCINTYRE M E, ROBERTSON A W. On the use and significance of is isentropic potential-vorticity maps [J]. Quart. J. Roy. Meteor. Soc., 1985, 111: 877-946.
[4] THORPE A J. Diagnosis of balanced vortex structure using potential vorticity [J]. J. Atmos. Sci., 1985, 42: 397-406.
[5] SHAPIRO L J. Hurricane Vortex Motion and Evolution in a Three-Layer Model [J]. J. Atmos. Sci., 1992, 49(2): 140-154.
[6] SHAPIRO L J, FRANKLIN J L. Potential Vorticity in Hurricane Gloria [J]. Mon. Wea. Rev., 1995, 123(5): 1465-1475.
[7] MOLINARI J, SKUBIS S, VOLLARO D. External Influences on Hurricane Intensity Part III: Potential Vorticity Structure [J]. J. Atmos. Sci., 1995, 52(20): 3593-3606.
[8] CHO H R, CAO Z H. Generation of Moist Potential Vorticity in Extratropical Cyclones Part II: Sensitivity to Moisture Distribution [J]. J. Atmos. Sci., 1998, 55: 595-610.
[9] DENG Guo, ZHOU Yu-shu, LI Jian-tong. The experiments of the boundary layer schemes on simulated typhoon part I. the effect on the structure of typhoon [J]. Chin. J. Atmos. Sci., 2005, 29: 417-428.
[10] GAO Shou-ting, LEI Ting, ZHOU Yu-shu. Diagnostic analysis of moist potential vorticity in torrential rain systems [J]. J. Appl. Meteor. Sci., 2002, 13: 662-670.
[11] GAO Shou-ting, LEI Ting, ZHOU Yu-shu. Moist potential vorticity anomaly with heat and mass forcings in torrential rain systems [J]. Chin. Phys. Lett.，2002, 19: 878-880.
[12] GAO S, WANG X, Zhou Y. Generation of generalized moist potential vorticity in a frictionless and moist adiabatic flow [J]. Geophy. Res. Lett., 2004, 31, L12113, doi: 10.1029/2003GL019152.
[13] GAO Shou-ting, ZHOU Yu-shu, CUI Xiao-peng. Impacts of cloud-induced mass forcing on the development of moist potential vorticity anomaly during torrential rains [J]. Adv. Atmos. Sci., 2004, 21(6): 923-927.
[14] GAO Shou-ting, ZHOU Yu-shu, LEI Ting, et al. Analyses of hot and humid weather in Beijing city in summer and its dynamical identification [J]. Sci. in China (Ser. D Earth Sci.), 2005, 48: 128-137.
[15] GAO S, CUI X, ZHOU Y, et al. A modeling study of moist and dynamic vorticity vectors associated with two-dimensional tropical convection [J]. J. Geophys. Res., 2005, 110, D17104, doi: 10.1029/2004JD005675.
[16] GAO S, RAN L K. Diagnosis of wave activity in a heavy-rainfall event [J]. J. Geophys. Res., 2009, 114, D08119, doi: 10.1029/2008JD010172.
[17] BENNETTS D A, HOSKINS B J, Conditional symmetric instability—A possible explanation for frontal rainbands [J]. Quart. J. Roy. Meteor. Soc., 1979, 105: 945-962.
[18] CAO Z, CHO H R. Generation of moist potential vorticity in extratropical cyclones [J]. J. Atmos. Sci., 1995, 52: 3263-3281.

Citation: DENG Guo and GAO Shou-ting. The theory of moist potential vorticity and its application in the diagnosis of typhoon rainfall and intensity. *J. Trop. Meteor.*, 2009, 15(2): 204-209.